IJP: Drugs and Drug Resistance 8 (2018) 518–525

Contents lists available at ScienceDirect

IJP: Drugs and Drug Resistance

journal homepage: www.elsevier.com/locate/ijpddr

Molecular and pharmacological characterization of an acetylcholine-gated chloride channel (ACC-2) from the parasitic nematode *Haemonchus contortus*

Sarah A. Habibi, Micah Callanan, Sean G. Forrester*

Applied Bioscience Graduate Program, Faculty of Science, University of Ontario Institute of Technology, 2000 Simcoe Street North, Oshawa, ON, L1H 7K4, Canada

ARTICLE INFO

Keywords:
Cholinergic receptor
Nicotinic acetylcholine receptors (nAChR)
Acetylcholine-gated chloride channel
Mutagenesis
Haemonchus contortus
Anthelmintic

ABSTRACT

Nematode cys-loop ligand-gated ion channels (LGICs) have been shown to be attractive targets for the development of novel anti-parasitic drugs. The ACC-1 family of receptors are a unique group of acetylcholine-gated chloride channels present only in invertebrates, and sequence analysis suggests that they contain a novel binding site for acetylcholine. We have isolated a novel member of this family, Hco-ACC-2, from the parasitic nematode *Haemonchus contortus* and using site-directed mutagenesis, electrophysiology and molecular modelling examined how two aromatic amino acids in the binding site contributed to agonist recognition. It was found that instead of a tryptophan residue in binding loop B, which essential for ligand binding in mammalian nAChRs, there is a phenylalanine (F200) in Hco-ACC-2. Amino acid changes at F200 to either a tyrosine or tryptophan were fairly well tolerated, where a F200Y mutation resulted in a channel hypersensitive to ACh and nicotine as well as other cholinergic agonists such as carbachol and methacholine. In addition, both pyrantel and levamisole were partial agonists at the wild-type receptor and like the other agonists showed an increase in sensitivity at F200Y. On the other hand, in Hco-ACC-2 there is a tryptophan residue at position 248 in loop C that appears to be essential for receptor function, as mutations to either phenylalanine or tyrosine resulted in a marked decrease in agonist sensitivity. Moreover, mutations that swapped the residues F200 and W248 (ie. F200W/W248F) produced non-functional receptors. Overall, Hco-ACC-2 appears to have a novel cholinergic binding site that could have implications for the design of specific anthelmintics that target this family of receptors in parasitic nematodes.

1. Introduction

The Cys-loop (cysteine-loop) superfamily of ligand-gated ion channels (LGICs) are a major class of receptor-coupled ion channels. These channels have been widely studied in invertebrate organisms for decades because they play key roles in the nervous system, making them prime targets for insecticides and nematocides (Del Castillo et al., 1963). The channel contains five protein subunits, encoded by the same or different subunit genes, all situated around a central aqueous pore. Each subunit contains an extracellular N-terminal ligand binding domain, where two cysteine residues, situated 13 amino acid residues apart, form a disulfide bond, as well as four transmembrane domains (TM1-TM4), and an extracellular C-terminus. These subunits can assemble as homo-oligomers, containing one subunit type, or hetero-oligomers, containing multiple subunit types (Sine and Engel, 2006).

Upon ligand binding, these channels elicit fast inhibitory or excitatory neurotransmission. In mammals, excitatory channels include nicotinic acetylcholine receptors (nAChRs) and 5-hydroxytryptamine (5-HT_3) serotonin receptors, and inhibitory channels include gamma-aminobutyric acid (GABA) and glycine receptors (Ortells and Lunt, 1995). Invertebrates, specifically parasitic and free-living nematodes, contain a variety of LGIC subunit types which are not found in vertebrates (Jones and Sattelle, 2008). These channels have been shown to be gated by neurotransmitters including GABA (Bamber et al., 1999; Siddiqui et al., 2010), glutamate (Cully et al., 1994), tyramine (Pirri et al., 2009), acetylcholine (ACh) (Putrenko et al., 2005), and serotonin (Ranganathan et al., 2000).

The ligand-binding site of cys-loop receptors is located at the interface of two adjacent subunits, which are loops A-C on the principal subunit and loops D-G on the complementary subunit (Hibbs and Gouaux, 2011). Each receptor has a different ligand-binding domain that contain various residues, which allow for the selection of different molecular agonists. There are key aromatic residues in the binding site of LGICs that have shown to be involved in ligand binding (Beene et al., 2004). Many neurotransmitters contain a cationic center that acts to stabilize the interaction between a cation and the negative electrostatic potential on the face of the aromatic ring. This is known as cation-π interactions (Beene et al., 2002). These cation- π interactions involve

* Corresponding author.
E-mail address: sean.forrester@uoit.ca (S.G. Forrester).

https://doi.org/10.1016/j.ijpddr.2018.09.004
Received 22 August 2018; Received in revised form 17 September 2018; Accepted 17 September 2018
Available online 22 September 2018

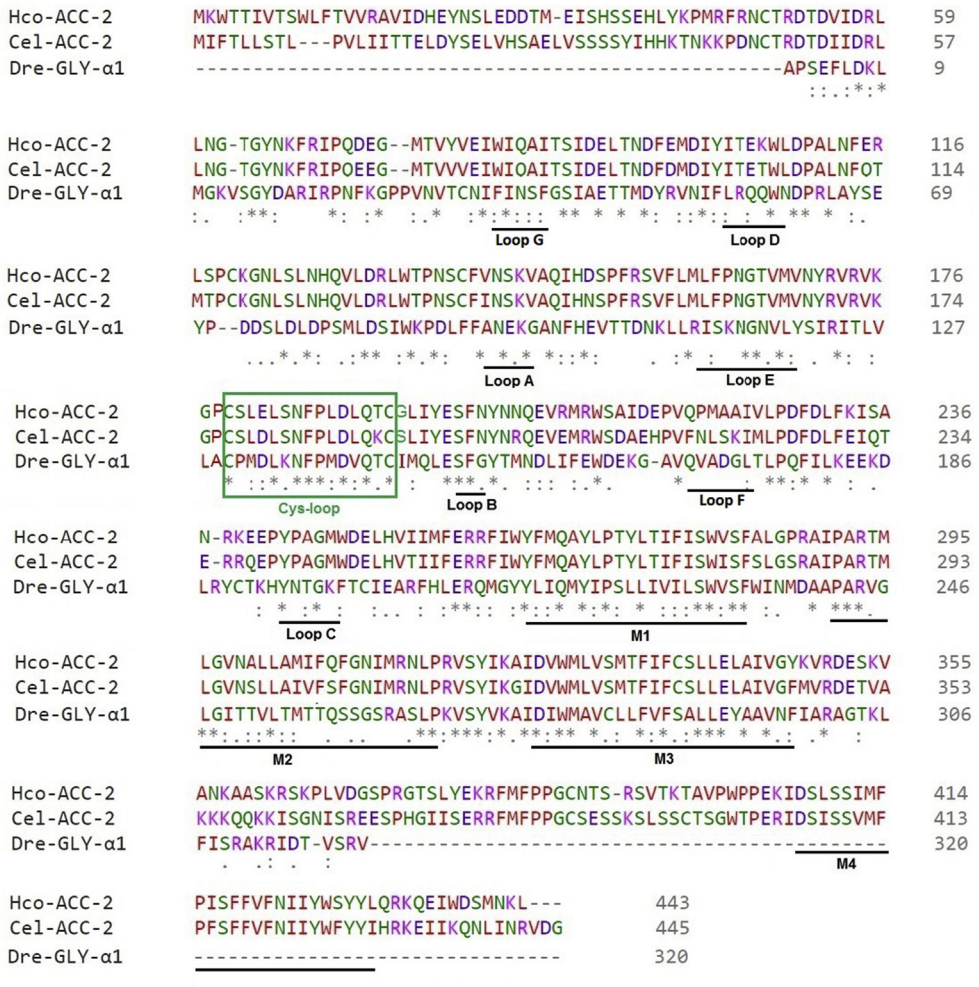

Fig. 1. Protein sequence alignment of the *H. contortus* Hco-ACC-2 receptor with *C. elegans* Cel-ACC-2 and *D. rerio* Dre-GLY-α1 receptors. All seven binding loops (Loop A-G), the characteristic cysteine residues that form the "cys-loop", and four transmembrane domains (M1-M4) and highlighted with underlines. (*) indicates identity and (:) indicates similarity.

aromatic amino acids (either phenylalanine, tyrosine, or tryptophan) in the ligand binding region (Dougherty, 1996). While the importance of aromatic residues for the function of the agonist binding pocket is widely shared across the phyla, there is variability across different receptors with respect the type of aromatic residues that contribute to binding and their location within the binding loops (Lynagh and Pless, 2014). This highlights the promiscuous nature of neurotransmitter binding across a variety of receptors in animals.

Early studies from the mollusk, *Aplysia,* reported the presence of a unique class of acetylcholine receptors in neurons, the acetylcholine-gated chloride channels (ACCs) (Kehoe and McIntosh, 1998). Later, studies identified these receptors in the model nematode *Caenorhabditis elegans* (Putrenko et al., 2005; Wever et al., 2015). In *C. elegans* the ACC-1 family is made up of eight receptor subunit genes*, acc-1, -2, -3*, and *-4,* and *lgc-46, -47, -48,* and *-49* (Jones and Sattelle, 2008). The sheep parasite, *Haemonchus contortus*, contains homologues for seven of the ACC-1 gene members, with the absence of *lgc-48* (Laing et al., 2013). As a whole, this family of receptors has potential to be novel antiparasitic drug targets. This is primarily due to the fact that they appear to be expressed in tissues that are sensitive to anthelmintic action, and as sequence analysis suggests, they are not present in mammals and exhibit a unique acetylcholine binding site (Putrenko et al., 2005; Wever et al., 2015). However, the structural components that are important for agonist recognition of this class of cholinergic receptors has not been explored.

Here we have isolated a novel member if the ACC-1 family (Hco-ACC-2) from the parasitic nematode *H. contortus* and investigated the binding site through site-directed mutagenesis and pharmacological analysis. Several introduced point mutations that changed key aromatic residues at the binding site revealed some interesting pharmacological properties. Molecular modelling was used to visualize the structure of the binding pocket and the interaction of key residues with a variety of agonists.

2. Methods

2.1. Isolation of hco-acc-2

H. contortus was received from Dr. Prichard (Institute of Parasitology, McGill University). Total RNA was extracted from adult male *H. contortus* using Trizol (Invitrogen, Carlsbad, USA). Complementary DNA (cDNA) was synthesized using the Quantitect Reverse Transcriptase kit from Qiagen (Dusseldorf, Germany), using a unique 3′ oligo-dT anchor primer sequence (5′CCTCTGAAGGTTCACG-GATCCACATCTAGATTTTTTTTTTTTTTTTTVN3′); [where V is either A, C, or G and N is either A, C, G, or T] (Weston et al., 1999). Gene specific primers were generated based on a partial sequence provided by Dr. Robin Beech (McGill University) as part of the genome sequencing project for *H. contortus* (Laing et al., 2013). The original sequence appeared to contain the full 3′end of the gene but was missing the 5′

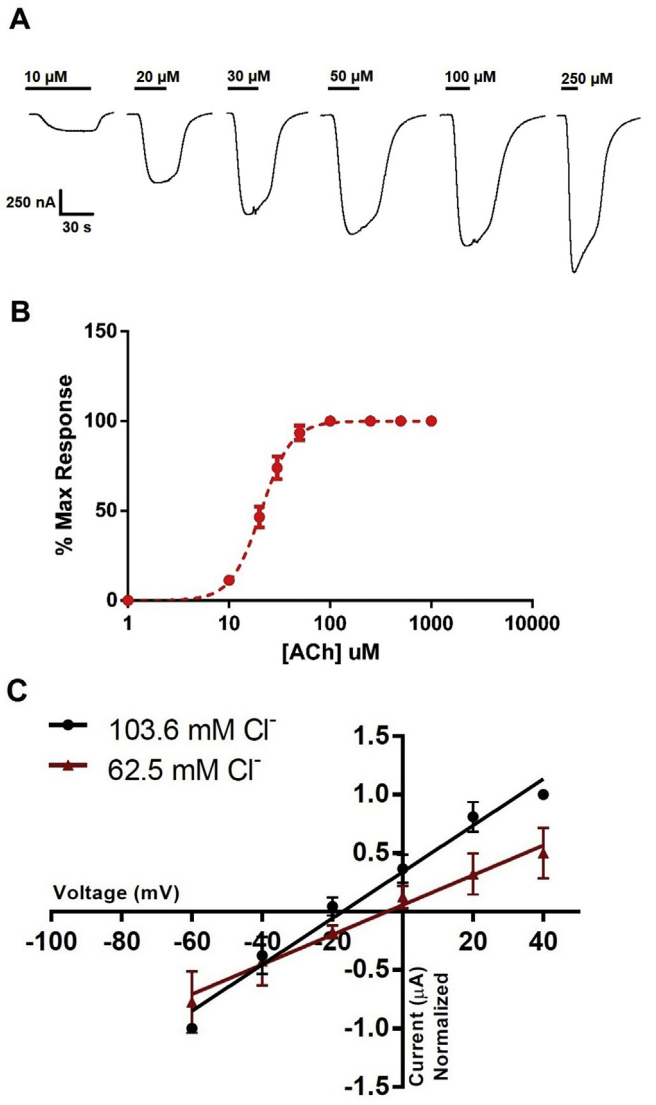

Fig. 2. Hco-ACC-2 is an acetylcholine-gated chloride channel. (A) Electrophysiological response of Hco-ACC-2 to increasing concentrations of ACh. (B) Dose-response curve for acetylcholine on the Hco-ACC-2 channel. Standard errors are shown. $n = 7$ oocytes (C) Current-voltage analysis of the Hco-ACC-2 channel using 103.6 mM Cl^- and 62.5 mM Cl^- in ND96 buffer solution. Acetylcholine response were generated using a maximum wild-type ligand saturation concentration of 250 μM. Standard errors are shown.

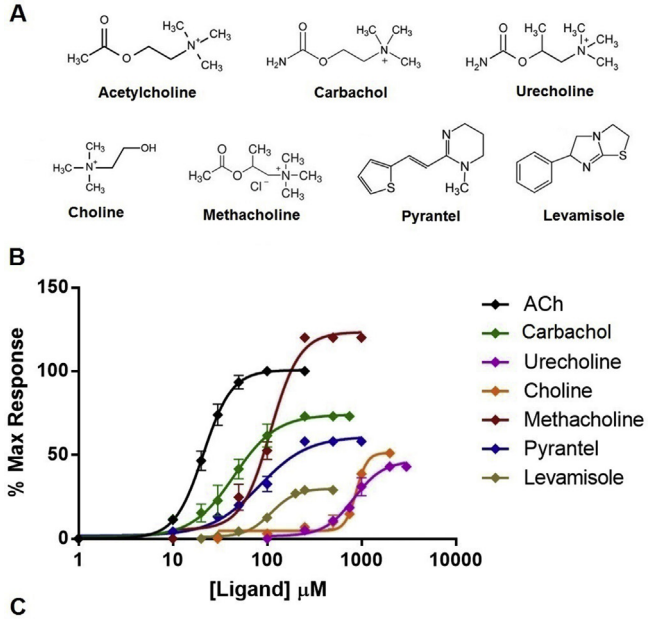

C

	EC_{50} ± SE (μM)	I_{MAX} (%)	n_H
Acetylcholine	20.86 ± 0.7	100	2.9
Pyrantel	71.70 ±3.5	58	1.7
Carbachol	43.0 ± 3.6	73	1.9
Levamisole	98.39 ± 4.0	29	3.1
Methacholine	100.4 ± 2.1	124	2.6
Urecholine	747.30 ± 22.4	43	2.9
Choline	1276.00 ± 34.8	51	2.8

Fig. 3. Pharmacology of Hco-ACC-2 (A) Chemical structures for the various molecular agonists used for the characterization of the Hco-ACC-2 binding site. (B) Dose-response curves for each of the listed compounds against the wild-type Hco-ACC-2 channel. Each curve is represented as a percent of the maximum acetylcholine response (250 μM). Partial agonists are those that have a maximum response lower than 100%. (C) Summary of the EC_{50} values ± standard error for each compound listed from most sensitive to least. I_{max} represents the maximal current response for each agonist.

region that would include the signal peptide cleavage site. The 5′ end of the gene was isolated using the 5′ rapid amplification of cDNA ends (RACE) protocol (Frohman et al., 1988). Two internal primers were used for the amplification of the 5′ end along with a primer specific for the splice-leader 1 sequence (SL1-5′-GGTTTAATTACCCAAGTTT GAG-3′) (Van Doren and Hirsh, 1988). The resulting amplicon of predicted size was isolated via a QIAquick Gel Extraction Kit (Qiagen, Dusseldorf, Germany) and sub-cloned into the pGEMT easy™ sequencing vector and was sequenced at Genome Quebec. Amplification of the complete *hco-acc-2* gene was carried out using primers specific to the 5′ and 3′ end of the gene with the XbaI and BamHI restriction sites and was subsequently cloned into the pGEMHE *Xenopus* expression vector (Zhang et al., 2008). All sequence alignments were produced using ClustalW.

2.2. Site-directed mutagenesis

The coding sequence of Hco-ACC-2 was sub-cloned into the pGEMHE transcription vector (3022 bp). The introduction of mutations in the Hco-ACC-2 coding sequence was performed using the QuikChange® II Site-Directed Mutagenesis Kit (Agilent Technologies). The primers carrying the specific mutation were generated using QuikChange Primer Design software from Agilent Technologies (QuikChange Primer Design). Five ACC-2 mutants were generated: F200Y, F200W, W248Y, W248F, and F200W/W248F. Point-mutations were confirmed using sequence analysis (Genome Quebec).

2.3. Expression in Xenopus laevis oocytes

All animal procedures followed the University of Ontario Institute of Technology Animal Care Committee and the Canadian Council on Animal Care guidelines. Expression of channels in oocytes was conducted as outlined in Abdelmassih et al. (2018). Female *Xenopus laevis* frogs were supplied by Nasco (Fort Atkinson, WI, USA). All frogs were housed in a climate controlled room (18 °C) with constant light cycling. Frogs were fed and tanks were cleaned regularly. Frogs were anesthetized with 0.15% 3-aminobenzoic acid ethyl ester methanesulphonate salt (MS-222) buffered with $NaHCO_3$ to pH 7 (Sigma-Aldrich, Oakville, ON, CA). Surgical removal of a section of the ovary of the frog was performed, and the lobe was defolliculated with a calcium-free oocyte Ringer's solution (82 mM NaCl, 2 mM KCl, 1 mM MgCl2, 5 mM HEPES pH 7.5 (Sigma-Aldrich)) (OR-2) containing 2 $mg{\cdot}mL^{1-}$ collagenase-II (Sigma-Aldrich). The oocytes in the defolliculation solution were

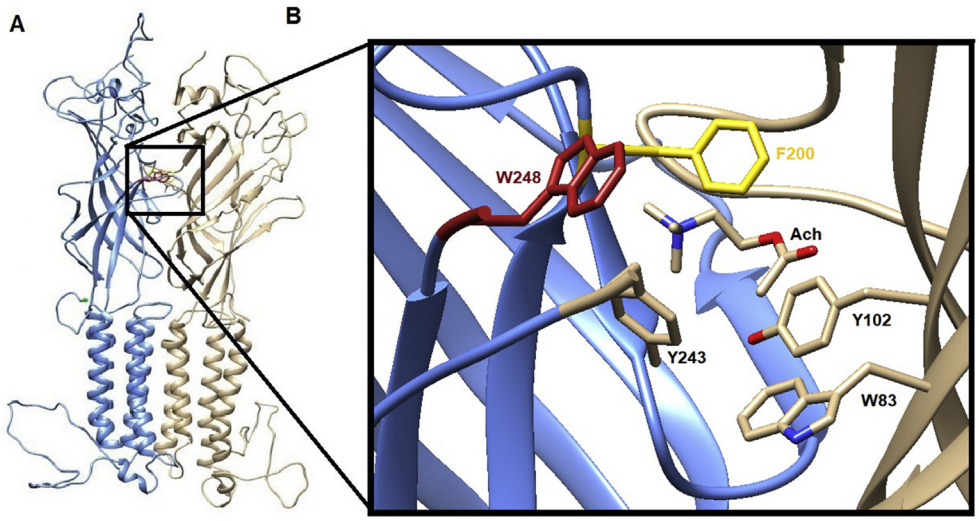

C

	Loop B					Loop C				
	200					248				
Hco-Acc-2	E	S	**F**	N	Y	G	M	**W**	D	E
Cel-ACC-2	E	S	**F**	N	Y	G	M	**W**	D	E
Cel-Deg-3	S	S	**W**	T	N	E	P	**W**	V	I
nAChR (human)	G	S	**W**	T	Y	E	I	**Y**	P	D
			*					*		

Fig. 4. (A) Homology model of Hco-ACC-2 homodimer. The principal and complementary subunits are represented by blue and beige respectively. (B) View of the Hco-ACC-2 binding pocket with acetylcholine docked. Key aromatic residues explored in this study, phenylalanine 200 (yellow) and tryptophan 248 (red) are highlighted. Other aromatic residues that may contribute to the binding site are also indicated. A portion of Loop C is removed from the image for clarity. (C) Protein alignment of the residues found in loop B and C of the Hco-ACC-2 with Cel-ACC-2, Cel-DEG-3 (GenBank accession # CAA98507.1), and the mammalian nAChR. * indicates the residue position for mutational analysis. (For interpretation of the references to colour in this figure legend, the reader is referred to the Web version of this article.)

incubated at room temperature for 2 h. Collagenase was washed from the oocytes with ND96 solution (1.8 mM $CaCl_2$, 96 mM NaCl, 2 mM KCl, 1 mM $MgCl_2$, 5 mM HEPES pH 7.5) and allowed one hour to recover at 18 °C in ND96 supplemented with 275 μg·mL^{1-} pyruvic acid (Sigma-Aldrich) and 100 μg·mL^{1-} of the antibiotic gentamycin (Sigma-Aldrich) (Supplemented ND96). Stage V and VI oocytes were selected for cytoplasmic injection of cRNA.

The pGEMHE vector containing the *hco-acc-2* coding sequence was linearized using the restriction enzyme PstI (New England Biolabs, USA), and used as template for an *in vitro* transcription reaction (T7 mMessage mMachine kit, Ambion, Austin, TX, USA) yielding *hco-acc-2* copy RNA. *X. laevis* oocytes were injected with 50 nl of *hco-acc-2* (0.5 ng·nL^{1-}) using the Drummond (Broomall, PA, USA) Nanoject microinjector. The expression of *hco-acc-2* required the co-injection with the copy RNA encoding three accessory proteins, *unc-50, unc-74, and ric-3.1* (Boulin et al., 2011) which were gifts from Dr. Cédric Neveu (INRA). The injected oocytes were incubated at 18 °C in supplemented ND96 solution. Electrophysiological recordings of the oocytes were conducted between 48 and 72 h after cRNA injection.

2.4. Electrophysiological recordings

Two-electrode voltage clamp electrophysiology was conducted using the Axoclamp 900A voltage clamp (Molecular Devices, Sunnyvale, CA, USA). Glass electrodes were produced using a P-97 Micropipette Puller (Sutter Instrument Co., Novato, CA, USA). The electrodes were backfilled with 3 M KCl and contained Ag|AgCl wires. The following molecules were first dissolved in ND96; Acetylcholine (ACh), Choline Chloride (Choline), Carbamoylcholine Chloride (Carbachol), Acetyl-β-methylcholine Chloride (Methacholine), Carbamyl-β-methylcholine chloride (Urecholine) [Sigma Aldrich], Levamisole Hydrochloride (Levamisole), and Pyrantel Citrate Salt (Pyrantel) [Santa Cruz Biotechnology]. These solutions were perfused over oocytes using the RC-1Z recording chamber (Warner Instruments Inc., Hamdan, CT, USA). Data was analyzed using Clampex Software v10.2 (Molecular Devices) and all graphs were generated using Graphpad Prism Software v5.0 (San Diego, CA, USA). EC_{50} values were determined by dose response curves that had been fitted to the following equation:

$$Imax = 1/\left[1 + \left(\frac{EC50}{[D]}\right)^{h}\right]$$

Where I_{max} is the maximal response, EC_{50} is the concentration of compound required to elicit 50% of the maximal response, [D] is compound concentration, and h is the Hill coefficient. Both EC_{50} and h are free parameters, and the curves were normalized to the estimated I_{max} using 250 μM ACh. Graphpad prism used the equation to fit a sigmoidal curve of variable slopes to the data. Means were determined from at least 5 oocytes from at least two batches of frogs. Significant differences between EC_{50} values comparing WT to mutants was performed using Student's T-test with the Bonferroni correction. *P*-values ≤ 0.01 were considered significant.

Current-voltage relationships were recorded by changing the holding potential from −60 mV to 40 mV in 20 mV increments. At each step the oocyte was exposed to a 250 μM concentration of ACh. For reduced Cl^- trials, NaCl was partially replaced by Na-gluconate (Sigma) in the ND96 buffer solution, for a final Cl^- concentration of 62.5 mM. Current-voltage graphs were generated using Graphpad Prism Software v5.0 (San Diego, CA, USA).

2.5. Homology modelling

The template used was the *Danio rerio* alpha-1 glycine receptor (3JAD) which showed the highest homology to Hco-ACC-2. The protein coding sequence of Hco-ACC-2 was aligned to template using SWISS-MODEL which was used in MODELLER v9.15 (Šali and Blundell, 1993) for the generation of the Hco-ACC-2 homodimer. The associated DOPE

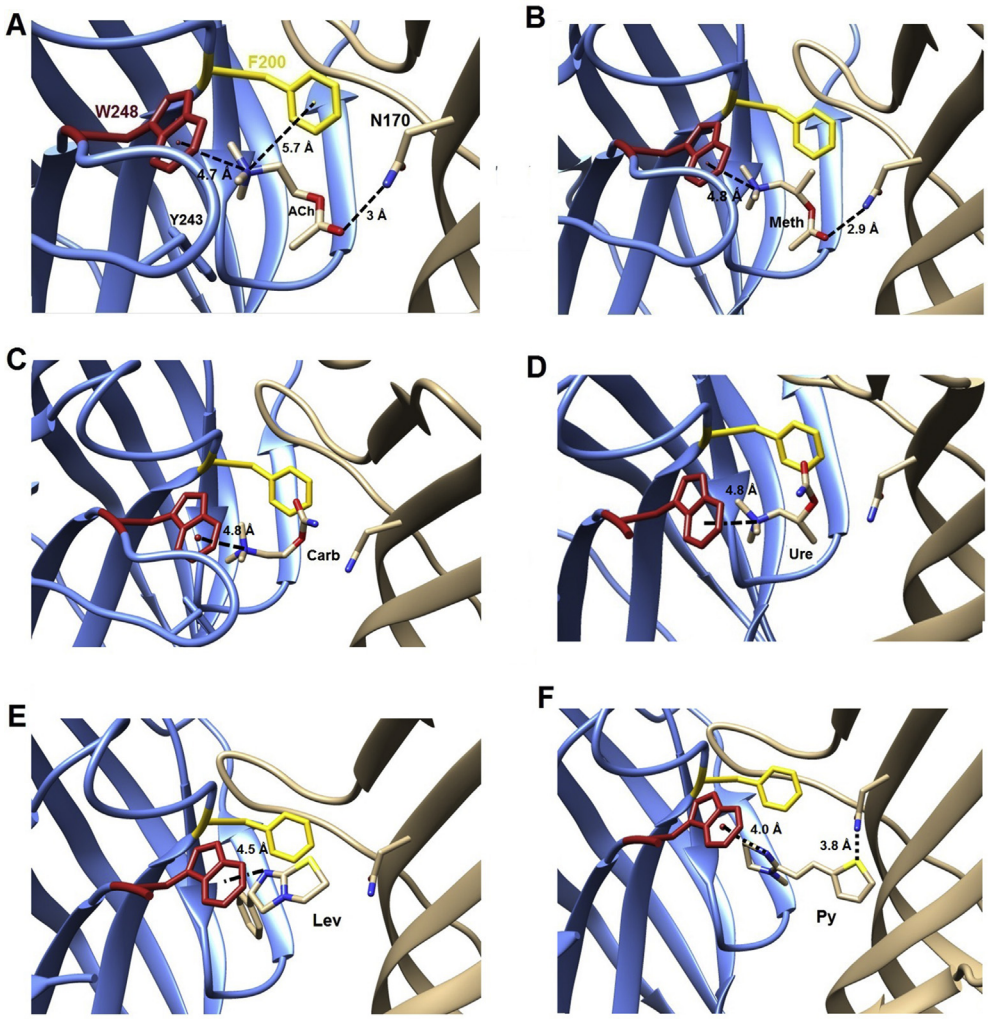

Fig. 5. Homology models of Hco-ACC-2 with docked agonists. (A) Acetylcholine (ACh) docked in the binding pocket of the Hco-ACC-2 receptor. Distance between the quaternary amine in ACh with W248 (4.7 Å) and F200 (5.7 Å) are represented by a dotted line and measured in angstroms (Å). Distance between N170 in loop E to the carbonyl oxygen in ACh (3 Å) is also shown. (B) Methacholine (Meth) docked in the Hco-ACC-2 binding pocket. W248 is 4.8 Å away from the quaternary amine of methacholine. N170 is 2.9 Å away from the carbonyl oxygen in methacholine. (C) Carbachol (Carb) docked in the Hco-ACC-2 binding pocket. W248 is 4.8 Å away from the quaternary amine in carbachol. (D) Urecholine (Ure) docked in the Hco-ACC-2 binding pocket. W248 is 4.8 Å away from the quaternary amine in urecholine. (E) Levamisole (Lev) docked in the Hco-ACC-2 binding pocket. (F) Pyrantel (Py) docked in the Hco-ACC-2 binding pocket.

and molpdf scores determined the most energetically favorable model. The final model chosen was visually inspected to ensure the binding loops were in the proper positions. Preparation of the homodimer for agonist docking was carried out using AutoDock Tools. Ligands including ACh and all of the molecules mentioned were obtained from the Zinc database in their energy-reduced extended form. AutoDock Vina was used to simulate docking of each ligand to the homodimers (Trott and Olson, 2010). Pymol was used to visualize the protein homodimer with its associated ligands, and Chimera v1.6.1 (Pettersen et al., 2004) was used to determine the distance between amino acid residues and ligand.

3. Results

3.1. Isolation of hco-acc-2

The full-length coding sequence of the *hco-acc-2* gene consisted of 1332 nucleotides (GenBank Accession # KC918364.1). When viewed in the appropriate reading frame, the sequence encodes for a protein containing 443 amino acids (AHM25234.1). The protein sequence contains a signal peptide cleavage site (Signal P; http://www.cbs.dtu.dk/services/SignalP/), all seven extracellular binding loops, four transmembrane domains, and the hallmark Cys-loop motif (Fig. 1). The Hco-ACC-2 protein sequences shares 88% similarity to the Cel-ACC-2 protein (Fig. 1). The PAR motif present at the beginning of the transmembrane 2 domain indicates anion selectivity through the channel (Jensen et al., 2002).

3.2. Expression of hco-acc-2 in Xenopus oocytes

Injection of *hco-acc*-2 cRNA alone did not result in ACh-sensitive channels. However, the injection of *X. laevis* oocytes with cRNA encoding *hco-acc-2,* and the accessory proteins, *hco-unc-74*, *hco-unc-50*, and *hco-ric-3.1*, resulted in a homomeric ACC-2 channel that was highly sensitive to ACh. ACh currents were in μA range, dose-dependent and desensitizing and were consistent in multiple oocytes from several frogs (Fig. 2A and B). In addition, current-voltage analysis of the Hco-ACC-2 channel was conducted to confirm anion selectivity through the channel. A full Cl^- concentration of ND96 (103.6 mM Cl^-) indicated a reverse potential of -17.44 ± 5 mV (n = 4). This is consistent with the calculated Nernst potential for Cl^- of -18.5 mV, when assuming an internal Cl^- concentration of 50 mM (Kusano et al., 1982). When NaCl was partially replaced with Na-gluconate (final Cl^- concentration of 62.5 mM) the reverse potential shifted to -3.4 ± 2 mV (n = 4), which is also consistent with the assumed Nernst potential of -5.7 mV (Fig. 2B).

3.3. Pharmacological analysis

Several cholinergic agonists and anthelmintics were examined. The EC_{50} value for ACh was 21 ± 0.7 μM (n = 7). The ACh analogue carbachol had an EC_{50} of 43 ± 3.6 μM (n = 6). Other ACh derivatives, including methacholine, urecholine, and choline also activated the channel with EC_{50} values of 100 ± 2 μM (n = 6), 747 ± 22 μM (n = 10), and 1276 ± 35 μM (n = 7), respectively. Currently used

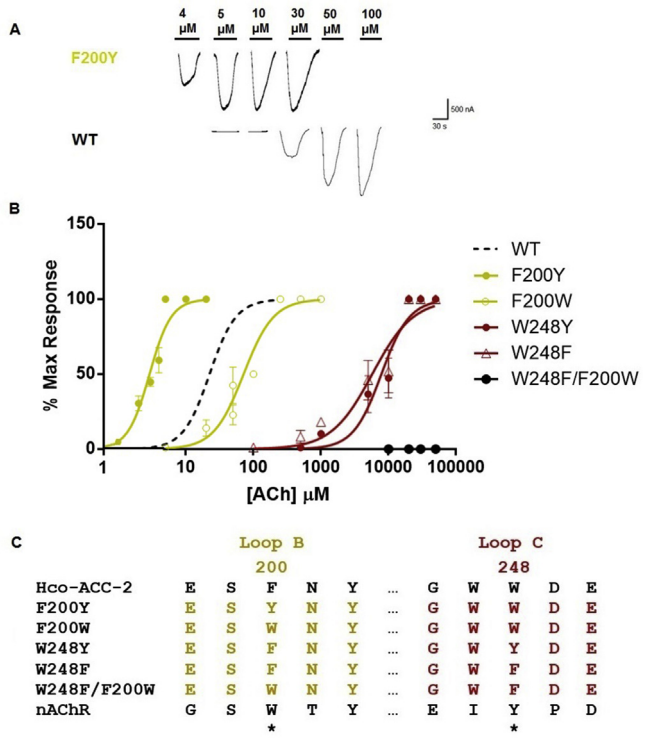

Fig. 6. Impact of mutations at key aromatic residues (A) Electrophysiological traces of the F200Y mutant compared to Hco-ACC-2 wild-type. (B) Dose-response curves for the WT and each of the mutated channels with acetylcholine. Loop B and C mutants are represented by yellow and red respectively. (C) Protein alignment of Loop B and C in the Hco-ACC-2 receptor for each of the generated mutants. * indicates the location of mutational analysis. (For interpretation of the references to colour in this figure legend, the reader is referred to the Web version of this article.)

anthelmintics such as pyrantel and levamisole were partial agonists for the receptor with EC_{50} values of 72 ± 4 µM (n = 6) and 98 ± 4 µM (n = 6) respectively. All pharmacological data is represented in Fig. 3. The compounds that showed to be full agonists were ACh and methacholine. All other compounds tested appeared to be partial agonists of the channel (Fig. 3).

3.4. Homology modelling

In order to visualize the interaction of agonists with residues in the binding pocket, a homology model was generated for the Hco-ACC-2 dimer using the *D. rerio* glycine receptor 3JAD as template which exhibited the highest homology with Hco-ACC-2. The model chosen, with the lowest DOPE score, is outlined in Fig. 4A. Cys-loop receptors are

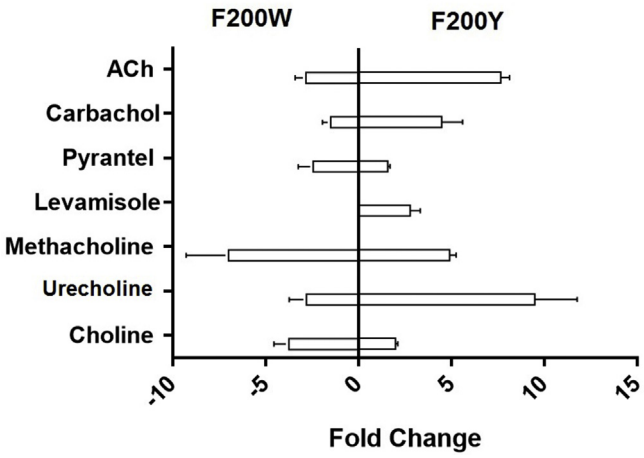

Fig. 7. Mutations at F200 have varying effects on agonist sensitivity. Fold changes in EC_{50} for the loop B mutants (F200Y and F200W) against all of the compounds listed. A positive fold change represents the channel becoming more sensitive to that compound, whereas a negative fold change represents the channel becoming less sensitive.

known to contain an aromatic box in the binding site. The binding site on the primary and complementary subunits appear to be composed of several aromatic residues. Based on sequence alignment of the Hco-ACC-2 protein with the mammalian nAChR, two aromatic residues in binding loops B and C appear to be swapped. The residues that appeared to interact with all agonists were phenylalanine 200 (F200) in loop B, and tryptophan 248 (W248) in loop C. The quaternary amine group in ACh was situated between 4.7 Å and 5.7 Å away from W248 and F200 respectively (Figs. 4B and 5A). The quaternary amine of other molecules such as carbachol, methacholine and urecholine also docked at a similar distance from the two aromatic residues (Fig. 5B, C and D). Partial agonists such as carbachol and urecholine docked in a bent formation (Fig. 5C and D). The anthelmintics levamisole and pyrantel also docked with their quaternary amine close to W248 (Fig. 5E and F). In addition, an asparagine residue (N170) in loop E is also present within the binding pocket, and its hydroxyl group is located 3 Å from the carbonyl oxygen in ACh. The equivalent position in the nAChR is L121 (β2 subunit) (Morales-Perez et al., 2016) which highlights another potential difference in the agonist binding site between ACCs and nAChRs. Methacholine which is also a full agonist docked in a similar orientation as ACh with its carbonyl oxygen within 3 Å from the NH_2 group of N170 (Fig. 5B). Since all agonists appear to dock with their quaternary amine between F200 and W248, these two residues were chosen for further analysis.

Table 1
Summary of EC_{50} values ± standard error for each channel with all of the compounds listed. N.R[a] indicates the channel did not respond to concentrations of indicated compound at concentrations ≥1 mM which is a concentration that elicited a maximal response on the WT channel. N.R[b] indicated that the channel did not respond to concentration up to 20 mM. $n \geq 5$ oocytes. NR = no response; ND = not determined.

	WT	F200Y	F200W	W248Y	W248F	F200W/W248F
Acetylcholine	21 ± 1	2.9 ± 0.1**	61 ± 4**	7854 ± 275*	5600 ± 1258*	N.R[b]
Carbachol	43 ± 4	9.7 ± 0.5**	67 ± 4	N.R[a]	N.R[a]	N.R[b]
Choline	1276 ± 35	650 ± 13**	4771 ± 543*	N.R[a]	N.R[a]	N.R[b]
Methacholine	100 ± 2	20 ± 1**	644 ± 84**	N.R[a]	N.R[a]	N.R[b]
Urecholine	747 ± 22	81 ± 3**	2151 ± 215**	N.R[a]	N.R[a]	N.R[b]
Levamisole	98 ± 4	39 ± 3**	N.D	N.R[a]	N.R[a]	N.R[b]
Pyrantel	72 ± 4	44 ± 2**	160 ± 20	N.R[a]	N.R[a]	N.R[b]

*indicates significant difference compared to WT ($P < 0.01$).
**indicates significant difference compared to WT ($P < 0.001$).
NOTE: For each molecule (row), statistical analysis compared EC_{50} values between WT and each mutant.

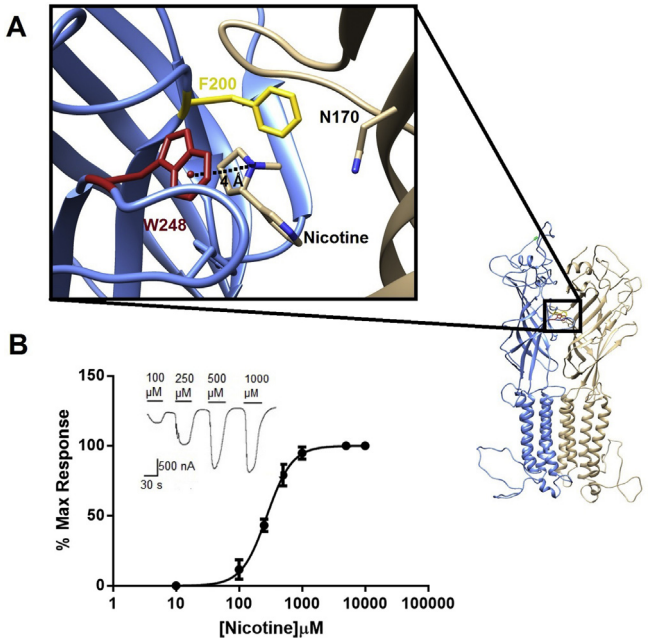

Fig. 8. (A) Nicotine docked in the Hco-ACC-2 WT binding pocket. The quaternary amine of nicotine is located 4 Å away from W248. (B) Dose-response curve for the F200Y mutant with nicotine. INSET: Electrophysiological traces of nicotine activation of Hco-ACC-2. $n = 5$ oocytes.

3.5. Mutational analysis

Five Hco-ACC-2 mutants were generated, including F200Y, F200W, W248Y, W248F, and F200W/W248F swap. When the phenylalanine (Phe) at position 200 was replaced with a tyrosine (Tyr) residue, the resulting channel became significantly more sensitive to ACh compared to wild-type (Fig. 6A). The EC_{50} of the F200Y channel was 3 ± 0.1 µM (n = 5) (Fig. 6B). The mutation of the Phe in loop B to a tryptophan (Trp) resulted in a channel that was slightly less sensitive to ACh, with an EC_{50} value of 72 ± 4 µM (n = 5) (Fig. 6B). Replacement of Trp at position 248 had a much larger negative impact on the channel, with EC_{50} values for ACh of 7854 ± 275 µM (n = 5) and 5600 ± 1258 µM (n = 6) for W248Y and W248F, respectively (Fig. 6B). These two mutants did not respond to any of the other compounds at the concentrations tested. The double swap mutation (F200W/W248F) resulted in a channel that was no longer responsive to ACh nor the other compounds (Table 1).

Both the F200Y and F200W single mutants were further characterized using the other agonists listed in Fig. 3A. The F200Y mutation was up to 9-fold more sensitive to all compounds listed, whereas the F200W mutation was up to 7-fold less sensitive (Fig. 7). It appears that both ACh and urecholine were most affected by the F200Y mutation whereas methacholine was most affected by F200W. On the other hand, the sensitivity of the anthelmintic pyrantel was only minimally affected by the two mutations. The resulting EC_{50} values for each compound is outlined in Table 1. The two Trp mutants, W248Y and W248F, did not respond to any of the other agonists (Table 1). Similarly the double mutant F200W/W248F did not respond to any of the agonists tested (Table 1).

3.6. Nicotine activates Hco-ACC-2 F200Y

The Hco-ACC-2 WT channel responded to nicotine at concentrations above 500 µM. It should be noted that some un-injected oocytes showed a small increase in current when exposed to 500 µM nicotine (Data not shown). Therefore, while we believe that the WT channel does respond to high concentrations of nicotine we did not determine an EC_{50}. However, since the F200Y mutant responded to lower concentrations of nicotine we conducted dose response experiments which revealed an EC_{50} of 277 ± 8 µM (n = 5) (Fig. 8B). Nicotine was docked in the binding pocket and its quaternary amine was situated 4 Å away from the center of the W248 benzene ring (Fig. 8A). The N2 quaternary amine in nicotine was 5.5 Å from the F200.

4. Discussion

We have identified a member of the ACC-1 family in the parasitic nematode *H. contortus* and investigated its binding site using site-directed mutagenesis, homology modelling and pharmacological analysis. This family of receptors appear to be unique to invertebrates and not present in mammals, making them attractive targets for novel nematocides. This has been validated by research demonstrating that this family of receptors are expressed in tissues that are sensitive to anthelmintic action (Wever et al., 2015). The research described here has examined in detail the structure of the ACC binding site which is important for future research focused on the discovery of novel therapeutics.

The pharmacology of the Hco-ACC-2 receptor can provide some valuable insight into the nature of the binding site. In our analysis, the receptor is least sensitive to choline. The low sensitivity of the receptor to choline is likely due to the molecules smaller size and lack of a carbonyl group which limits its interaction with residues. These features could explain why, compared to the other agonists, there was very little change in sensitivity of choline in the hypersensitive mutant F200Y. Moreover, the comparison between the sensitivities of ACh, carbachol, methacholine and urecholine along with the molecular docking results highlights some interesting trends. For example, all molecules docked with their quaternary amine close to W248. However, both ACh and methacholine, which exhibited maximum efficacy, appear to dock in a similar extended orientation, which places them within 3 Å of N170. On the other hand, carbachol and urecholine, which are both partial agonists, dock in a similar bent orientation, which is more pronounced in urecholine, and places them further away from N170.

One of the key features of ACh binding to mammalian nAChR is the presence of a tryptophan residue that participates in π-cationic interactions with the quaternary amine on ACh. In mammalian nAChRs this tryptophan residue is present in loop B (Beene et al., 2002). However, in ACC receptors there is no tryptophan residue in loop B. Instead, sequence analysis and homology modelling reveal a tryptophan residue present in loop C (W248). W248 is facing into the binding pocket and appears to be within 5 Å of the quaternary amine of the agonists that were docked in this study. While we did not confirm that W248 is participating in a π-cationic interaction with agonists, it is clear that it is essential for the function of Hco-ACC-2. Evidence for the importance of W248 in the function of ACC receptors is highlighted by mutational analysis, which showed that changing W248 to either W248Y or W248F resulted in a severely impacted receptor that did not respond to any agonists other than ACh. This could be partially explained by the removal of the indole nitrogen which is found in tryptophan. The presence of an indole nitrogen causes a large negative electrostatic cloud around this residue, allowing for increased potential of π-cationic interactions (Mecozzi et al., 1996). Since this indole is not present in tyrosine or phenylalanine, it could explain why these mutations were detrimental to receptor function. In addition, the positioning of this tryptophan in loop C could be important in ACC receptor function, as swapping the residues from loop C to B (F200W/W248F) produced a non-functional channel. This phenomenon is reminiscent of the novel nematode 5-HT receptor MOD-1 which also has a tryptophan residue in loop C instead of loop B, as seen in 5-HT_3 receptors (Ranganathan et al., 2000). The loop C tryptophan in the MOD-1 receptor was shown to participate in the essential π-cationic interaction with serotonin which is key for receptor binding (Mu et al., 2003). Interestingly, this loop C

tryptophan is not only present in ACC and MOD-1 receptors but other amine-gated chloride channels such as LGC-55 (tyramine) (Rao et al., 2010) and LGC-53 (dopamine) (Beech et al., 2013) as well as the nematode DEG-3 receptor (Fig. 3). From, an evolutionary perspective it appears that the presence of a tryptophan in loop C is an essential requirement for a diverse array of nematode cys-loop receptors, and their ability to bind to wide range of ligands.

Unlike mammalian nAChRs which exhibit a tryptophan in loop B, the Hco-ACC-2 receptor exhibits a phenylalanine (F200). Mutations at this position provided some additional insight into the structure of the ACC binding site. First, the introduction of a F200W change caused a reduced sensitivity to all agonists, albeit to varying degrees. Carbachol was the least affected by the change while methacholine was most affected. Methacholine is a full agonist for the ACC receptor and differs from ACh with the addition of a methyl group in the backbone, but both appear to bind in a similar orientation in the wildtype receptor. The addition of a bulky tryptophan residue may therefore cause the larger methacholine to shift orientation and reducing its ability to bind and activate the channel. Interestingly, the opposite was found with the F200Y mutation, which increased the sensitivity of all agonists (including nicotine) to varying degrees. Here, urecholine exhibited the highest increase in sensitivity. It is possible the hydroxyl group on tyrosine allows additional hydrogen-bond interactions with surrounding residues, thus changing the structure of the binding site and enhancing agonist (especially urecholine) binding. F200 may also have other roles such as participating in π-cationic interactions with agonists. However, future experiments would have to confirm.

The ACC receptor family appear to be attractive targets for the development of novel anthelmintics. With this in mind we also tested the activity of the anthelmintics levamisole and pyrantel which activate the nematode nAChR (Martin and Robertson, 2007). We found both molecules were partial agonists for the Hco-ACC-2 receptor. However, we were surprised to observe that the mutations we introduced into the receptor minimally effected in their activity. This may highlight the distinct manner at which these anthelmintics bind to the ACC receptors. Molecular models for docked pyrantel and levamisole place both molecules within 5 Å of W248. However, the overall positioning of levamisole and pyrantel within the ACC-2 binding site are clearly different (Fig. 5). How this relates to the differences in efficacy we observed between the two molecules requires further examination.

This study has described the isolation of a member of the ACC family from *H. contortus* and examined two residues in the binding site that are important for agonist recognition. Further research on the essential requirements for agonist recognition of ACC receptor can provide insight into the evolution of cholinergic neurotransmission and may possibly lead to the discovery of novel cholinergic anthelmintics.

Declarations of interest

None.

Acknowledgements

This research was funded by grants from Natural Sciences and Engineering Research Council of Canada (Grant #210290) and the Canadian Foundation for Innovation to SGF. The authors declare no conflicts of interest.

References

Abdelmassih, S.A., Cochrane, E., Forrester, S.G., 2018. Evaluating the longevity of surgically extracted Xenopus laevis oocytes for the study of nematode ligand-gated ion channels. Invertebr. Neurosci. 18, 1.

Bamber, B.A., Beg, A.A., Twyman, R.E., Jorgensen, E.M., 1999. The Caenorhabditis elegans unc-49 locus encodes multiple subunits of a heteromultimeric GABA receptor. J. Neurosci. 19, 5348–5359.

Beech, R.N., Callanan, M.K., Rao, V.T.S., Dawe, G.B., Forrester, S.G., 2013. Characterization of cys-loop receptor genes involved in inhibitory amine neurotransmission in parasitic and free living nematodes. Parasitol. Int. 62, 599–605.

Beene, D.L., Brandt, G.S., Zhong, W., Zacharias, N.M., Lester, H.A., Dougherty, D.A., 2002. Cation− π interactions in ligand recognition by serotonergic (5-HT3A) and nicotinic acetylcholine receptors: the anomalous binding properties of nicotine. Biochemistry 41, 10262–10269.

Beene, D.L., Price, K.L., Lester, H.A., Dougherty, D.A., Lummis, S.C.R., 2004. Tyrosine residues that control binding and gating in the 5-hydroxytryptamine3 receptor revealed by unnatural amino acid mutagenesis. J. Neurosci. 24, 9097–9104.

Boulin, T., Fauvin, A., Charvet, C.L., Cortet, J., Cabaret, J., Bessereau, J., Neveu, C., 2011. Functional reconstitution of Haemonchus contortus acetylcholine receptors in Xenopus oocytes provides mechanistic insights into levamisole resistance. Br. J. Pharmacol. 164, 1421–1432.

Del Castillo, J., Morales, T.A., Sanchez, V., 1963. Action of piperazine on the neuromuscular system of Ascaris lumbricoides. Nature 200, 706.

Cully, D.F., Vassilatis, D.K., Liu, K.K., Paress, P.S., Van der Ploeg, L.H., Schaeffer, J.M., et al., 1994. Cloning of an avermectin-sensitive glutamate-gated chloride channel from Caenorhabditis elegans. Nature 371, 707.

Van Doren, K., Hirsh, D., 1988. Trans-spliced leader RNA exists as small nuclear ribonucleoprotein particles in Caenorhabditis elegans. Nature 335, 556.

Dougherty, D.A., 1996. Cation-pi interactions in chemistry and biology: a new view of benzene, Phe, Tyr, and Trp. Science 80 (271), 163.

Frohman, M.A., Dush, M.K., Martin, G.R., 1988. Rapid production of full-length cDNAs from rare transcripts: amplification using a single gene-specific oligonucleotide primer. Proc. Natl. Acad. Sci. Unit. States Am. 85, 8998–9002.

Hibbs, R.E., Gouaux, E., 2011. Principles of activation and permeation in an anion-selective Cys-loop receptor. Nature 474 (7349), 54–60.

Jensen, M.L., Timmermann, D.B., Johansen, T.H., Schousboe, A., Varming, T., Ahring, P.K., 2002. The β subunit determines the ion selectivity of the GABAA receptor. J. Biol. Chem. 277, 41438–41447.

Jones, A.K., Sattelle, D.B., 2008. The cys-loop ligand-gated ion channel gene superfamily of the nematode, *Caenorhabditis elegans*. Invertebr. Neurosci. 8, 41–47.

Kehoe, J., McIntosh, J.M., 1998. Two distinct nicotinic receptors, one pharmacologically similar to the vertebrate α7-containing receptor, mediate Cl currents in Aplysia neurons. J. Neurosci. 18, 8198–8213.

Kusano, K., Miledi, R., Stinnakre, J., 1982. Cholinergic and catecholaminergic receptors in the Xenopus oocyte membrane. J. Physiol. 328, 143–170.

Laing, R., Kikuchi, T., Martinelli, A., Tsai, I.J., Beech, R.N., Redman, E., et al., 2013. The genome and transcriptome of Haemonchus contortus, a key model parasite for drug and vaccine discovery. Genome Biol. 14, R88.

Lynagh, T., Pless, S.A., 2014. Principles of agonist recognition in Cys-loop receptors. Front. Physiol. 24 (5), 160.

Martin, R.J., Robertson, A.P., 2007. Mode of action of levamisole and pyrantel, anthelmintic resistance, E153 and Q57. Parasitology 134, 1093–1104.

Mecozzi, S., West Jr., A.P., Dougherty, D.A., 1996. Cation-pi interactions in aromatics of biological and medicinal interest: electrostatic potential surfaces as a useful qualitative guide. Proc. Natl. Acad. Sci. U. S. A. 93 (20), 10566–10571.

Morales-Perez, C.L., Noviello, C.M., Hibbs, R.E., 2016. X-ray structure of the human α4β2 nicotinic receptor. Nature 538, 411.

Mu, T.-W., Lester, H.A., Dougherty, D.A., 2003. Different binding orientations for the same agonist at homologous receptors: a lock and key or a simple wedge? J. Am. Chem. Soc. 125, 6850–6851.

Ortells, M.O., Lunt, G.G., 1995. Evolutionary history of the ligand-gated ion-channel superfamily of receptors. Trends Neurosci. 18, 121–127.

Pettersen, E.F., Goddard, T.D., Huang, C.C., Couch, G.S., Greenblatt, D.M., Meng, E.C., et al., 2004. UCSF Chimera—a visualization system for exploratory research and analysis. J. Comput. Chem. 25, 1605–1612.

Pirri, J.K., McPherson, A.D., Donnelly, J.L., Francis, M.M., Alkema, M.J., 2009. A tyramine-gated chloride channel coordinates distinct motor programs of a Caenorhabditis elegans escape response. Neuron 62, 526–538.

Putrenko, I., Zakikhani, M., Dent, J.A., 2005. J. Biol. Chem. 280, 6392–6398.

Ranganathan, R., Cannon, S.C., Horvitz, H.R., 2000. MOD-1 is a serotonin-gated chloride channel that modulates locomotory behaviour in C. elegans. Nature 408, 470–475.

Rao, V.T.S., Accardi, M.V., Siddiqui, S.Z., Beech, R.N., Prichard, R.K., Forrester, S.G., 2010. Characterization of a novel tyramine-gated chloride channel from Haemonchus contortus. Mol. Biochem. Parasitol. 173, 64–68.

Šali, A., Blundell, T.L., 1993. Comparative protein modelling by satisfaction of spatial restraints. J. Mol. Biol. 234, 779–815.

Siddiqui, S.Z., Brown, D.D.R., Rao, V.T.S., Forrester, S.G., 2010. An UNC-49 GABA receptor subunit from the parasitic nematode Haemonchus contortus is associated with enhanced GABA sensitivity in nematode heteromeric channels. J. Neurochem. 113, 1113–1122.

Sine, S.M., Engel, A.G., 2006. Recent advances in Cys-loop receptor structure and function. Nature 440, 448–455.

Trott, O., Olson, A.J., 2010. AutoDock Vina: improving the speed and accuracy of docking with a new scoring function, efficient optimization, and multithreading. J. Comput. Chem. 31, 455–461.

Weston, D., Patel, B., Van Voorhis, W.C., 1999. Virulence in Trypanosoma cruzi infection correlates with the expression of a distinct family of sialidase superfamily genes. Mol. Biochem. Parasitol. 98, 105–116.

Wever, C.M., Farrington, D., Dent, J.A., 2015. The validation of nematode-specific acetylcholine-gated chloride channels as potential anthelmintic drug targets. PLoS One 10, e0138804.

Zhang, J., Xue, F., Chang, Y., 2008. Structural determinants for antagonist pharmacology that distinguish the ρ1 GABAC receptor from GABAA receptors. Mol. Pharmacol. 74, 941–951.